

High time resolution observations of HF cross-modulation within the *D* region ionosphere

J. Langston¹ and R. C. Moore¹

Received 17 March 2013; accepted 20 March 2013; published 30 May 2013.

[1] High-frequency cross-modulation is employed to probe the *D* region ionosphere during HF heating experiments at the High-frequency Active Auroral Research Program (HAARP) observatory. We have adapted Fejer's well-known cross-modulation probing method to determine the extent of ionospheric conductivity modification in the *D* region ionosphere with high (5 μ .sec) time resolution. We demonstrate that the method can be used to analyze *D* region conductivity changes produced by HF heating both during the initial stages of heating and under steady state conditions. The sequence of CW probe pulses used allow the separation of cross-modulation effects that occur as the probe pulse propagates upward and downward through the heated region. We discuss how this probing technique can be applied to benefit ELF/VLF wave generation experiments and ionospheric irregularities experiments at higher altitudes. We demonstrate that large phase changes equivalent to Doppler shift velocities >60 km/s can be imposed on HF waves propagating through the heated *D* region ionosphere. **Citation:** Langston, J., and R. C. Moore (2013), High time resolution observations of HF cross-modulation within the *D* region ionosphere, *Geophys. Res. Lett.*, 40, 1912–1916, doi:10.1002/grl.50391.

1. Introduction

[2] Ionospheric cross-modulation experiments have been used to probe the lossy lower ionosphere for over 50 years [e.g., Fejer, 1955, 1970; Weisbrod *et al.*, 1964; Senior *et al.*, 2010]. The cross-modulation effect was first observed by Tellegen [1933], who established that the modulation of one signal could be transferred to another signal propagating within the same patch of ionospheric plasma (i.e., the *Luxembourg Effect*). Cross-modulation occurs because one signal modifies the electron temperature of the collisional *D* region ionosphere, in turn modifying the rate of absorption experienced by the second signal [e.g., Huxley and Ratcliffe, 1949]. Measurements of the cross-modulated signal can be used to quantify the heater-modified characteristics of the *D* region ionosphere, and the technique (pioneered by Fejer [1955]) has been explored extensively [e.g., Fejer, 1970; Weisbrod *et al.*, 1964; Senior *et al.*, 2010]. The method uses a sequence of short, high-power disturbing pulses and short, low-power probing pulses, precisely timed so that the

probe pulse reflects from the *F* region and is cross modulated only as it propagates downward through the modified *D* region, allowing the virtual interaction altitude to be directly calculated.

[3] Although pulsed cross-modulation is a well-established science, for a large class of HF heating experiments, the ionosphere is heated for long periods of time and does not recover to its ambient state between heating pulses. Fejer's method cannot be applied in such cases because the probe pulse would experience cross-modulation during both of its *D* region traverses. One such class of prolonged-duration experiments is the generation of extremely low frequency (ELF, 3–3000 Hz) and very low frequency (VLF, 3–30 kHz) waves by modulated HF heating [e.g., Getmantsev *et al.*, 1974; Stubbe *et al.*, 1982]. Observations of ELF/VLF waves generated in this manner sensitively depend on the strength of the electrojet currents, the properties of the Earth-ionosphere waveguide, and the modulation of *D* region conductivity by HF heating [e.g., Stubbe *et al.*, 1982; Rietveld *et al.*, 1986; Golkowski *et al.*, 2009]. In practice, it can be difficult to distinguish the relative importance of these various effects for a given transmission, particularly as a function of the ELF/VLF frequency. The HF cross-modulation experiments described herein can be used to provide an independent measurement of the conductivity modulation during ELF/VLF wave generation experiments because HF cross-modulation does not depend on the electrojet field strength or on the Earth-ionosphere waveguide.

[4] Another example is the generation of ionospheric irregularities in the *E* and *F* region ionospheric layers. The generation of ionospheric irregularities typically requires relatively long (more than several seconds) duration CW heating pulses. Many types of irregularities exhibit HF power thresholds for excitation [e.g., Hysell *et al.*, 2011; Mahmoudian *et al.*, 2013]. Proper analysis of the power thresholds supplied in these works depends on the level of ambient and heater-modified absorption in the *D* region ionosphere. Accurate assessment of the HF power thresholds for excitation of the irregularities requires accurate assessment of *D* region absorption at the HF employed.

[5] This paper presents a method to quantify High-frequency Active Auroral Research Program (HAARP)-modified *D* region absorption during long-duration CW and modulated HF heating experiments with high time resolution. We present HF cross-modulation observations that highlight well-established *D* region nonlinearities, including HF self-absorption effects, which produce different rates of absorption during the initial heating stages than during steady state conditions [e.g., Huxley and Ratcliffe, 1949] and conductivity saturation effects, which manifest as significant

¹Department of Electrical and Computer Engineering, University of Florida, Gainesville, Florida, USA.

Corresponding author: J. Langston, Department of Electrical and Computer Engineering, University of Florida, 570 NEB, PO Box 116130, Gainesville, FL 32611, USA. (langstonj@ufl.edu)

deviations from power-law dependence at high HF power levels [e.g., Moore *et al.*, 2006]. We also present new observations that demonstrate HAARP HF heating can produce rapid and significant HF signal phase changes, and we interpret these observations in terms of an equivalent Doppler shift velocity with HF radar application.

2. Description of the Experiment

[6] On 15 November 2012, the 3.6 MW HAARP HF transmitter located near Gakona, Alaska (62.39°N, 145.2°W) performed dual-beam HF cross-modulation experiments. The 12×15 element HAARP transmitter array was split evenly in the east-west direction to create two sub-arrays. The east array broadcast the modifying beam at 3.25 MHz (*X*-mode) with 78 dBW effective radiated power (ERP) while the west array broadcast the probe pulses at 4.5 MHz (*X*-mode) with 74 dBW ERP (at 10% power). During these transmissions, the HAARP digisonde indicated virtual reflection altitudes of 225–250 km for the 4.5 MHz (*X*-mode) probing pulses.

[7] In order to allow the separation of the cross-modulation effects that occur as the probe wave propagates upward and downward through the *D* region ionosphere, each of the beams followed a detailed schedule. Every 20 ms, the modifying beam was off for 6 ms, broadcast a short portion of a modulated waveform at full power, and then was off again for the remainder of the 20 ms period. The duration of the modulated waveform started at 20 μ s and increased in 5 μ s steps each 20 ms period (to a 5015 μ s duration during the last 20 ms period).

[8] Similarly, the probing beam operated on a tight 20 ms schedule. Every 20 ms, the probing beam broadcast three 10 μ s pulses at 10% power. The first pulse was always broadcast at the beginning of the 20 ms period (0 delay). The second pulse was broadcast with a 3 ms delay, and this delay increased by 5 μ s every 20 ms period (ending with a 7.995 ms delay during the final 20 ms period). The third pulse was broadcast with a 6 ms delay, and this delay increased by 5 μ s every 20 ms period (ending with an 10.995 ms delay during the final 20 ms period). Figure 1 shows a cartoon diagram of the transmission sequence for three different 20 ms periods.

[9] Using this transmission format, the upward and downward propagating cross-modulation can be separated. As depicted schematically in Figure 1, the first pulse acts as an ambient reference pulse that does not experience cross-modulation effects. The second pulse is initially not modulated (top panel), but as the second pulse delay increases, it is modulated as it propagates downward through the ionosphere (middle panel) and later as it propagates both upward and downward through the *D* region ionosphere (bottom panel). In all panels, the third pulse is modulated only as it propagates upward through the *D* region ionosphere, and it is broadcast together with the end of the modulated portion of the modifying HF beam. With this transmission sequence in mind, we can take the signal measurements of our probe pulses to be expressed as follows:

$$P_1 = A_1 e^{j\phi_1} \quad P_2 = A_2 e^{j\phi_2} \quad P_3 = A_3 e^{j\phi_3} \quad (1)$$

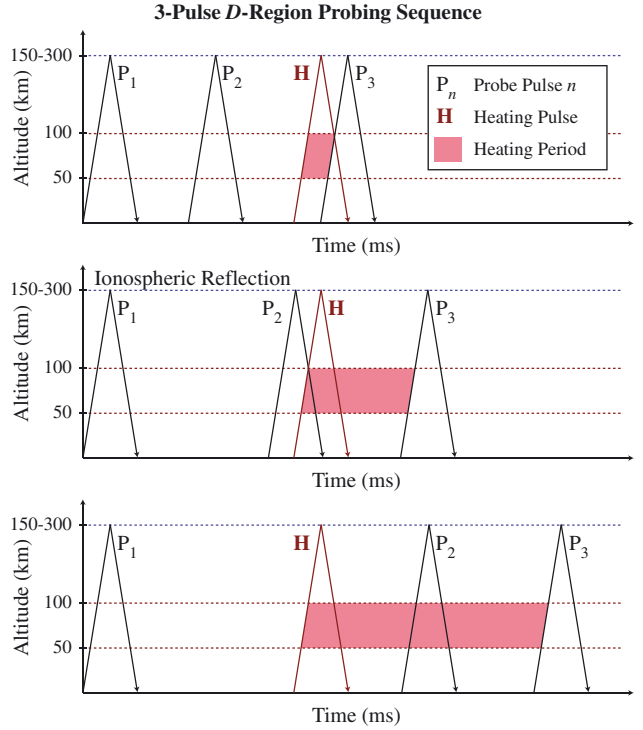


Figure 1. Bounce diagram of the three-pulse cross-modulation sequence at three different times. (top) Early (P_2 unmodulated). (middle) Mid-sequence (P_2 modulated as it propagates downward). (bottom) Late (P_2 modulated as it propagates upward and downward).

where the subscript indicates the pulse number. The amplitude and phase of the upward and downward propagating cross-modulation may then be expressed as

$$M_{\text{up}}(t) = \frac{P_3(t)}{P_1}, \quad M_{\text{down}}(t) = \begin{cases} \frac{P_2(t)}{P_1} & t < T_m \\ \frac{P_2(t)}{P_3(t)} & t \geq T_m \end{cases} \quad (2)$$

where t is the time delay at which the respective pulse was transmitted and T_m is the start time of the modulated beam transmission (i.e., 6 ms). In this manner the upward and downward propagating cross-modulation effects (particularly for $t \geq T_m$) can be isolated.

[10] This schedule was designed for six different modulation waveforms: 2.5 kHz sinusoidal AM (full power), 2.5 kHz sinusoidal AM (10% power), 2.5 kHz square wave AM (full power), 2.5 kHz square wave AM (10% power), 10.0 kHz sinusoidal AM (full power), and CW (full power). In order to produce consistent observations among the various waveforms, we interleaved the modulation waveforms (and their corresponding probing pulses) every 20 ms period.

[11] HF observations were performed at Oasis (OA, 62.35°N, 145.1°W, 3 km from HAARP). The HF receiving system consists of two orthogonal 90 ft folded dipoles located approximately 12 ft above the ground. The receiver is sensitive to electric fields with frequencies between 1.0 and 10.0 MHz, and data acquisition was performed continuously at 25 MHz with 14-bit resolution. Accurate timing is provided by GPS. Probe pulse measurements were performed in post processing. The signals from the two antennas were complex-summed (taking one antenna to be real valued and the other antenna to be imaginary valued)

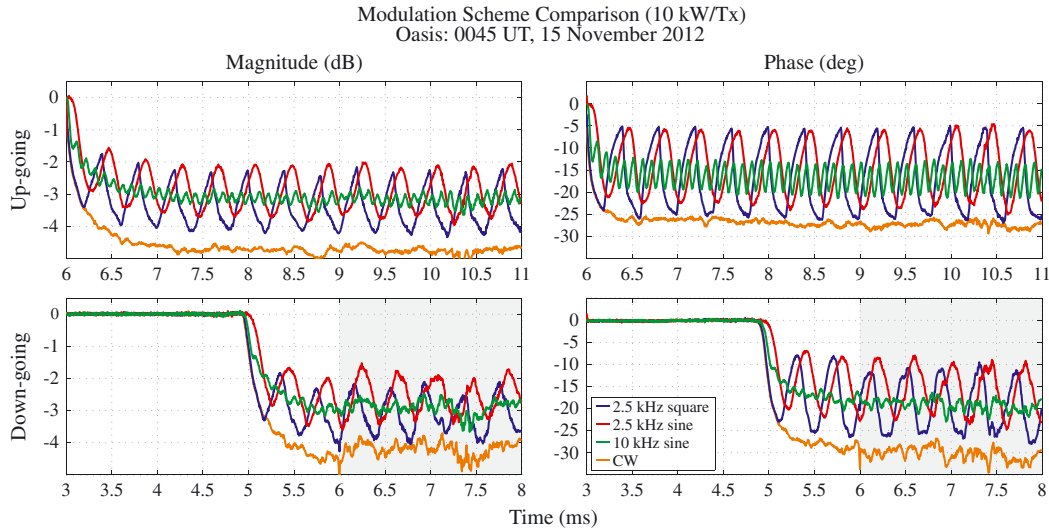


Figure 2. (left) Cross-modulation magnitude (dB) and (right) cross-modulation phase (degrees) for (top) upward propagation and (bottom) downward propagation for each modulation waveform.

in order to identify the X -mode component. The resulting signal was mixed down at 4.5 MHz and filtered using a zero-phase 10 kHz low-pass filter. The amplitude of the ionospherically reflected probe pulse is determined by detecting the maximum amplitude of the electric field shortly following the transmission. The phase of the ionospherically reflected probe pulse is taken to be the phase measured at the same time as the maximum amplitude.

3. Experimental Observations and Analysis

[12] Figure 2 shows experimental observations of M_{up} and M_{down} as a function of time for the four modulation waveforms employed. The traces closely align with expectations from a physical standpoint. The CW heating traces decrease rapidly (nearly exponentially) as a function of time, and they act as lower bounds for the modulation induced by AM heating. At steady state, the CW heating trace exhibits a 4–5 dB increase in absorption for both upward and downward propagating cross-modulation, while the phase exhibits a 28–30° decrease. As expected, the square wave and sinusoidal heating traces also exhibit rapid initial decreases, although they oscillate at the ELF/VLF frequency about an average value. The square wave heating traces closely follow the CW heating traces during the first heating cycle—the transmissions are the same during this time period—and the shape of the oscillation is almost triangular due to the heating and cooling rates. The 2.5 kHz square wave AM heating produces slightly larger (~ 0.5 dB, $\sim 5^\circ$) oscillations than sinusoidal AM heating, roughly consistent with ELF/VLF wave generation observations. The oscillations produced by 10 kHz sinusoidal AM heating are roughly 1.6 dB smaller than those produced by 2.5 kHz heating, and the 10 kHz cross-modulation is bounded on both sides by the 2.5 kHz cross-modulation. All of these observations are generally consistent with D region HF heating models that account for the full time evolution of the conductivity modulation [e.g., James, 1985].

[13] In all cases, the downward propagating cross-modulation calculation nearly seamlessly transitions at the 6 ms mark, demonstrating the approximate validity of the

new technique separating upward and downward propagating cross-modulation effects. The success of the technique is in part due to the validity of the approximation that the third pulse consists only of upward propagating cross-modulation. We evaluate this approximation here. Assuming the maximum altitude for D region interactions is ~ 100 km, the 225–250 km virtual reflection altitudes indicate that the third probe pulse will have an 0.83–1.00 ms delay between D region traverses. Examining the CW trace in close detail, an e -folding heating time scale of ~ 90 μs can be derived using the magnitude and ~ 50 μs can be derived using the phase. These values are on the same order of magnitude as the D region heating timescales derived by Barr and Stubbe [1991b], who also estimated corresponding cooling time scales to be on the order of 0.1 ms, which is 8–10 times

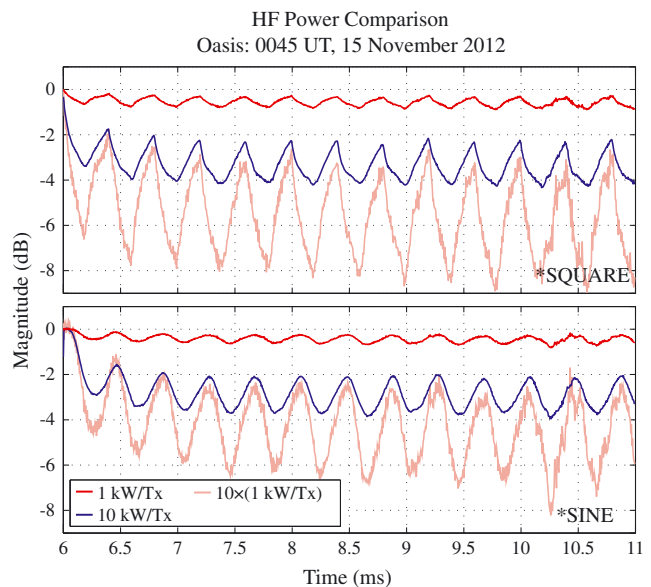


Figure 3. Cross-modulation magnitude (dB) at 10% (red) and 100% (blue) HF power for (top) square wave AM and (bottom) sinusoidal AM. The pink traces are the 10% HF power traces multiplied by a factor of 10, for reference.

smaller than the third pulse propagation delay between D region traverses. Even with somewhat larger cooling time scales, it would be reasonable to assume that the third pulse consists only of upward propagating cross-modulation.

[14] Having demonstrated that the new method successfully separates upward and downward propagating cross-modulation effects, it is instructive to investigate cross-modulation effects as a function of HF power. Figure 3 compares sinusoidal AM heating and square wave AM heating at peak HF power levels of 10% and 100%. It has been suggested that at low HF power levels, the conductivity modulation exhibits a power-law relationship with the HF power: $\sigma \propto (P_{\text{HF}})^n$, with n near 1 [Barr and Stubbe, 1991a]. In this case, the amplitude of cross-modulation observed at full power would be e^{10^n} times greater than at 10% power. This is a multiplicative factor of 10^n on decibel scale. For this reason, in Figure 3, we provide a third trace that represents the 10% decibel-scale power traces magnified by a factor of 10. As shown in Figure 3, the ratio of the 10% power trace to the 100% power trace is not constant as a function of time; during both square wave and sinusoidal AM heating, the ratio decreases during periods within the modulation cycle with higher HF power, consistent with the saturation effect first observed by Moore *et al.* [2006] during ELF/VLF wave generation experiments. Although only the upward propagating cross-modulation amplitudes are shown, each of the other components exhibits similar effects.

[15] Other types of conductivity modulation effects are also readily apparent in this data set. For instance, significant HAARP-modified phase changes can occur rapidly in time, as shown in Figure 2. The rapidly varying phase is produced by HAARP modulating the real part of the ionospheric refractive index. Although one could argue that HAARP HF heating could be modulating the F region reflection height (thereby modulating the phase), the observed propagation delays for the probe pulses do not support this conclusion. For this data set, the rapid temporal variation in phase is equivalent to several hundreds of Hertz variation in frequency, even for the CW modulation waveform. It is interesting to note that some HF radars use Doppler techniques to determine the range and speed of targeted objects. In this context, we can quantify the equivalent Doppler shifts that can be imposed upon an ionospherically propagating HF signal by HAARP HF heating. Due to the geometry of our experiment (i.e., vertical incidence), we expect the equivalent Doppler shifts we measure to be maximized: HF signals propagating at oblique angles through the heated region would experience different cross-modulation phasing that could be destructive, resulting in smaller Doppler shifts. Nevertheless, the equivalent observed Doppler shift velocity is

$$v(t) = \frac{-c\Delta f(t)}{f_0 + \Delta f(t)} \quad \text{with} \quad \Delta f(t) = \frac{1}{2\pi} \frac{d\psi(t)}{dt} \quad (3)$$

where $\psi(t)$ is the cross-modulation phase, c is the speed of light, and f_0 is 4.5 MHz.

[16] Figure 4 presents the equivalent Doppler shift velocity imposed on the 4.5 MHz probing pulses by the four modulation waveforms at full power. The Doppler shift equivalent velocity varies between -40 and $+69$ km/s, with details depending on the modulation waveform. For lower power (10%) heating (not shown), this velocity varied between -10.5 and $+9.5$ km/s. Based on these calculations,

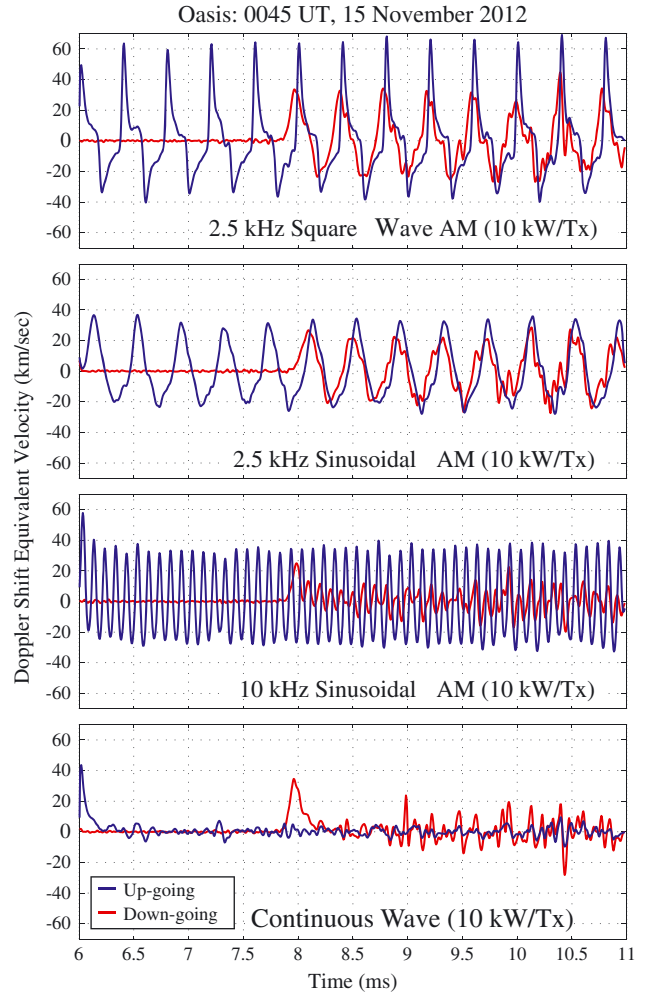


Figure 4. Effective Doppler shift velocity on the 4.5 MHz probe signal due to ionospheric heating using four different modulation waveforms at 100% power.

it is evident that significant Doppler shifts can be introduced on HF signals by ionospheric modification, even by the CW modulation waveform. As a result, it is possible that measurements of emissions produced at higher altitudes by CW heating could be affected by the rapidly varying conductivity of the D region, if they propagate downward through the region within $250\text{--}500 \mu\text{s}$. It is also of great interest to note that naturally occurring ionospheric disturbances, such as lightning-induced electron precipitation [e.g., Cotts *et al.*, 2011] and transient luminous events [e.g., Marshall *et al.*, 2006], are expected to produce much larger conductivity changes in the lower ionosphere than HF heating. We suggest that it may be possible for natural ionospheric disturbances to produce significant Doppler shifts on ionospherically propagating HF signals, interfering with HF radar operations.

4. Summary and Discussion

[17] The observations presented in Figure 2 demonstrate the successful implementation of three-pulse probing to quantify and isolate upward and downward propagating HF cross-modulation during long transmissions. We have applied the technique to demonstrate that CW heating using

the equally split HAARP array can produce 4–5 dB of HAARP-modified absorption. This experiment could be adjusted to quantify HAARP-modified absorption at higher ERP levels. Furthermore, using Figure 3, we definitively identified the ionospheric conductivity as the physical quantity that exhibits characteristics consistent with a saturation effect at high HF power levels. Lastly, we demonstrated that HAARP can induce rapid and significant phase changes equivalent to large Doppler shifts on ionospherically propagating HF waves.

[18] **Acknowledgments.** This work is supported by US Air Force grant FA9453-12-1-00246, DARPA contract HR0011-09-C-0099, DARPA grant HR0011-10-1-0061, and NSF grants AGS-0940248 and ANT-0944639 to the University of Florida.

[19] The Editor thanks Morris Cohen and Mike Kosch for their assistance in evaluating this paper.

References

- Barr, R., and P. Stubbe (1991a), ELF radiation from the Tromsø “Super Heater” facility, *Geophys. Res. Lett.*, *18*, 1035–1038.
- Barr, R., and P. Stubbe (1991b), On the ELF generation efficiency of the Tromsø heater facility, *Geophys. Res. Lett.*, *18*, 1971.
- Cotts, B. R. T., M. Gołkowski, and R. C. Moore (2011), Ionospheric effects of whistler waves from rocket-triggered lightning, *Geophys. Res. Lett.*, *38*, L24805, doi:10.1029/2011GL049869
- Fejer, J. A. (1955), The interaction of pulsed radio waves in the ionosphere, *J. Atmos. Terr. Phys.*, *7*, 322.
- Fejer, J. A. (1970), Radio wave probing of the lower ionosphere by cross-modulation techniques, *J. Atmos. Terr. Phys.*, *32*, 597.
- Getmantsev, C. G., et al. (1974), Combination frequencies in the interaction between high-power short-wave radiation and ionospheric plasma, *JETP Lett.*, *20*, 101–102.
- Gołkowski, M., U. S. Inan, and M. B. Cohen (2009), Cross modulation of whistler mode and HF waves above the HAARP ionospheric heater, *Geophys. Res. Lett.*, *36*, L15103, doi:10.1029/2009GL039669.
- Huxley, L. G. H., and J. A. Ratcliffe (1949), A survey of ionospheric cross-modulation, *Proc. Inst. Elec. Eng.*, *96*, 433–440.
- Hysell, D. L., E. Nossa, and M. McCarrick (2011), X-mode suppression of artificial E region field-aligned plasma density irregularities, *Rad. Sci.*, *46*, RS2010.
- James, H. G. (1985), The ELF spectrum of artificially modulated D/E-region conductivity, *J. Atmos. Terr. Phys.*, *47*(11), 1129–1142.
- Mahmoudian, A., et al. (2013), Ion gyro-harmonic structuring in the stimulated radiation spectrum and optical emissions during electron gyro-harmonic heating, *J. Geophys. Res. Space Physics*, *118*, doi:10.1002/jgra.50167.
- Marshall, R. A., U. S. Inan, and W. A. Lyons (2006), On the association of early/fast very low frequency perturbations with sprites and rare examples of VLF backscatter, *J. Geophys. Res.*, *111*, D19108, doi:10.1029/2006JD007219.
- Moore, R. C., U. S. Inan, and T. F. Bell (2006), Observations of amplitude saturation in ELF/VLF wave generation by modulated HF heating of the auroral electrojet, *Geophys. Res. Lett.*, *33*, L12106, doi:10.1029/2006GL025934.
- Rietveld, M. T., H. Kopka, and P. Stubbe (1986), D-region characteristics deduced from pulsed ionospheric heating under auroral electrojet conditions, *J. Atmos. Terr. Phys.*, *48*, 311–326.
- Senior, A., M. T. Rietveld, M. J. Kosch, and W. Singer (2010), Diagnosing radio plasma heating in the polar summer mesosphere using cross modulation: Theory and observations, *J. Geophys. Res.*, *115*, A09318, doi:10.1029/2010JA015379.
- Stubbe, P., H. Kopka, M. T. Rietveld, and R. L. Dowden (1982), ELF and VLF generation by modulated HF heating of the current carrying lower ionosphere, *J. Atmos. Terr. Phys.*, *44*, 1123–1135.
- Tellegen, B. D. H. (1933), Interaction between radio waves, *Nature*, *131*, 840.
- Weisbrod, S., A. J. Ferraro, and H. S. Lee (1964), Investigation of phase interaction as a means of studying the lower ionosphere, *J. Geophys. Res.*, *69*, 2337.